# Comparison of Calibration Techniques for Ground-Based C-Band Radiometers

Kai-Jen C. Tien, *Student Member, IEEE*, Roger D. De Roo, *Member, IEEE*, Jasmeet Judge, *Senior Member, IEEE*, and Hanh Pham, *Student Member, IEEE*

***Abstract*—We quantify the performance of three commonly used techniques to calibrate ground-based microwave radiometers for soil moisture studies, external (EC), tipping-curve (TC), and internal (IC). We describe two ground-based C-band radiometer systems with similar design and the calibration experiments conducted in Florida and Alaska using these two systems. We compare the consistency of the calibration curves during the experiments among the three techniques and evaluate our calibration by comparing the measured brightness temperatures ($T_B$'s) to those estimated from a lake emission model (LEM). The mean absolute difference among the $T_B$'s calibrated using the three techniques over the observed range of output voltages during the experiments was 1.14 K. Even though IC produced the most consistent calibration curves, the differences among the three calibration techniques were not significant. The mean absolute errors (MAE) between the observed and LEM $T_B$'s were about 2–4 K. As expected, the utility of TC at C-band was significantly reduced due to transparency of the atmosphere at these frequencies. Because IC was found to have a MAE of about 2 K that is suitable for soil moisture applications and was consistent during our experiments under different environmental conditions, it could augment less frequent calibrations obtained using the EC or TC techniques.**

***Index Terms*—Calibration, microwave radiometry, soil moisture.**

## I. Introduction

GROUND-BASED microwave radiometers have been used extensively to measure upwelling terrain emission in field experiments for hydrology, agriculture, and meteorology [1]–[7]. The total-power radiometer is of the simplest design compared to other designs such as Dicke and noise injection [8] and [9]. The stability and consistency of the relation between the output voltage and the antenna temperature, i.e., system gain and offset, are critical for radiometer operations. The system gain is highly sensitive to fluctuations in the physical temperature inside the radiometer requiring frequent calibration during radiometer operation for reliable and accurate observations.

Many calibration techniques have been developed for microwave radiometers for spaceborne and airborne [10]–[16] and ground-based radiometers [17]–[21]. In general, calibration techniques include observations of radiometer output voltages for cold and hot targets with known brightness temperatures [8], [9]. For radiometers operating at low frequencies away from the water vapor and oxygen absorption bands, such as C-band (6.7 GHz), commonly used cold targets are liquid nitrogen or the sky. Hot targets include microwave absorbers or matched loads inside the radiometers. For a C-band ground-based microwave radiometer, the conceptually simplest calibration technique using a microwave absorber at ambient temperature as a hot target is called "external calibration" (EC). Another widely used calibration technique that utilizes the sky measurements at different angles to calculate the optical depth of the atmosphere and the brightness temperatures of the sky is called "tipping curve calibration" (TC) [18], [19], [21]. Either EC or TC can be used exclusively, or TC could be used to provide a better estimate of the sky measurement for EC. Both techniques are inconvenient to perform frequently for long-term soil moisture studies using ground-based C-band radiometers. Moreover, the utility of TC at C-band might be hampered by the high atmospheric transparency at low microwave frequencies [8]. Another technique, "internal calibration" (IC), uses an internal matched load as the hot target. This technique has been used for spaceborne microwave radiometers, e.g., SMMR [10], TMR [13], [14], and JMR [15], airborne radiometers [16], and ground-based radiometers [17]. Unlike EC and TC, IC can be performed faster than gain fluctuation. Also, IC is neither sensitive to operator technique, to weathering of the delicate microwave absorber, nor does it require any additional hardware exclusively for the purpose of calibration. However, IC does not account for the losses in the antenna and transmission lines before the internal switch used to observe the matched load.

In this letter, we quantify the performance of IC and validate it using EC and TC for long-term observations of soil moisture using two ground-based C-band radiometers. Our analysis is restricted to horizontal polarization (H-pol) because of its higher sensitivity to soil moisture than vertical polarization (V-pol) [8]. We describe two ground-based total-power radiometers with similar design: the University of Florida C-band Microwave Radiometer (UFCMR) and the C-band unit on the Truck Mounted Radiometer System 3 (TMRS-3C), as well as the calibration experiments conducted under significantly different

Manuscript received June 5, 2006; revised September 29, 2006. This work was supported in part by the National Aeronautics and Space Administration's ESS Graduate Student Fellowship (ESSF03-0000-0044) and in part by the University of Florida, Institute of Food and Agricultural Sciences.

K.-J. C. Tien and J. Judge are with the Center for Remote Sensing, Department of Agricultural and Biological Engineering, University of Florida, Gainesville FL 32611 USA (e-mail: ktien@ufl.edu; jasmeet@ufl.edu).

R. D. De Roo is with the Department of Atmospheric, Oceanic, and Space Sciences, University of Michigan, Ann Arbor, MI 48109 USA (e-mail: deroo@umich.edu).

H. Pham is with the Department of Electrical Engineering and Computer Science, University of Michigan, Ann Arbor, MI 48109 USA (e-mail: hpham@umich.edu).

Color versions of one or more of the figures in this paper are available online at http://ieeexplore.ieee.org.

Digital Object Identifier 10.1109/LGRS.2006.886420

TABLE I
RADIOMETER SPECIFICATIONS FOR UFCMR AND TMRS-3C

| Parameter | | Value |
|---|---|---|
| Antenna type | Potter Horn | |
| Frequency | Center | 6.7 GHz |
| Bandwidth | 3 dB | 20 MHz |
| Beamwidth | 3 dB V-pol elev & azim | 23° & 21° |
| | 3 dB H-pol elev & azim | 21° & 23° |
| Isolation | | > 27 dB |
| Polarizations | Sequential | V/H |
| Noise Figure | From $T_{rec}$ | 3.99 dB |
| RF gain | | 85 dB |
| NEDT | 1 sec | 0.71 K |
| | 8 sec | 0.25 K |
| First Side-lobe | 47° from bore-sight | -26 dB |

environmental conditions in Florida and Alaska. We briefly summarize three different calibration techniques and compare the consistency of the calibration among these techniques using the two radiometers. We also discuss absolute accuracy of our brightness observations by comparing the observed brightness temperatures of a lake with those obtained using a lake emission model (LEM).

## II. C-BAND RADIOMETERS

The UFCMR and TMRS-3C were developed by the Microwave Geophysics Group at the University of Michigan (UM-MGG). Both are dual-polarized unbalanced total-power radiometers operating at the center frequency of 6.7 GHz near the frequency of the Advanced Microwave Scanning Radiometer—EOS (AMSR-E) aboard the NASA Aqua Satellite. The UFCMR is mounted on a 10-m tower, whereas the TMRS-3C is mounted on a Norstar truck's hydraulic arm, which can extend to 12 m. TMRS-3 consists of a suite of dual-polarized radiometers operating at 1.4, 6.7, 19, and 37 GHz mounted on an elevation positioner that allows for approximately 300° rotation in the elevation axis. A major difference between the UFCMR and TMRS-3C designs is the use of two receivers for V- and H-pol in TMRS-3C, compared to only one receiver in the UFCMR that switches between the two polarizations. Table I lists the specifications of the C-band radiometers.

## III. FIELD EXPERIMENTS

### A. Microwave Water and Energy Balance Experiments (MicroWEXs)

MicroWEXs were conducted by the Center for Remote Sensing, Department of Agricultural and Biological Engineering, University of Florida, at the Plant Science Research and Education Unit (PSREU), IFAS, Citra, FL, during the growing seasons of cotton (MicroWEX-1 [22] and -3 [23]) and corn (MicroWEX-2 [24]). During the MicroWEXs, the UFCMR measured microwave brightness temperatures every 15 min and was calibrated every two weeks. We conducted 10, 4, and 11 calibrations during the 140, 80, and 190 days of the MicroWEX-1, 2, and 3, respectively. Each calibration included measurements of sky at zenith angles of 15°, 30°, 45°, and 60°, of a microwave absorber at ambient temperature, and of a matched load inside the radiometer.

### B. Tenth Radiobrightness and Energy Balance Experiment (REBEX-10)

REBEX-10 was conducted by the UM-MGG from May 6 to July 1, 2004, at a site about 1 km north of Toolik Field Station on the North Slope of Alaska. In addition to conducting twice daily EC calibrations during REBEX-10, validation data were obtained by driving the Norstar truck to a beach on the northeast shore of Toolik Lake and extending the radiometer systems over the open water on June 21 (DOY 173) and 22 (DOY 174). The boom was extended to the west from the shore in the direction of the smallest solid angle of land presented at the opposite shore of the lake. The calibration targets included sky, absorber, and lake surface. The sky measurements were recorded at zenith angles of 0°, 10°, 23°, 30°, 32°, 40°, and 55°. The lake surface measurements were obtained at incidence angles of 23°, 30°, 32°, 40°, and 55°. The lake temperature was measured on DOY 173 at 1502 h (AKDT) to be 13.7 °C and on DOY 174 at 0342 h (AKDT) to be 10 °C. These are expected to be extreme lake temperatures during this period.

## IV. CALIBRATION METHODOLOGY

The relationship between the output voltage ($V_{\text{out}}$) and the antenna apparent temperature ($T'_B$) of a total-power radiometer with a square-law detector such as the UFCMR and the TMRS-3C can be expressed as follows:

$$T'_B = S \cdot V_{\text{out}} + I \tag{1}$$

where $S$ and $I$ are the slope and intercept of the calibration curve, respectively.

### A. External Calibration

The calibration targets of EC included the microwave absorber at ambient air temperature and the sky measurement at zenith angle of 15° for UFCMR and 0° for TMRS-3C. The $S$ and $I$ are

$$S = \frac{(T_{B,\text{sky}} - T_{\text{abs}}) \cdot \eta + (T_{\text{ant,sky}} - T_{\text{ant,abs}}) \cdot (1-\eta)}{V_{\text{out,sky}} - V_{\text{out,abs}}} \tag{2}$$

$$I = T_{B.\text{sky}} \cdot \eta + T_{\text{ant,sky}} \cdot (1-\eta) - S \cdot V_{\text{out,sky}} \tag{3}$$

where $T_{\text{abs}}$ is the physical temperature of the absorber (Kelvin), $\eta$ is the antenna efficiency, equal to 0.86 ± 0.01, as estimated in the laboratory using one-port measurements with a network analyzer, $T_{\text{ant,sky}}$ and $T_{\text{ant,abs}}$ are the physical temperatures of antenna during the sky and absorber measurements, respectively (Kelvin), and $V_{\text{out,sky}}$ and $V_{\text{out,abs}}$ are the output voltages during the sky and absorber measurements, respectively (volts). $T_{B,\text{sky}}$ (Kelvin) given by [8] is

$$T_{B,\text{sky}} = T_{B,\text{atm}}(\theta) + T_{\text{extra}} \cdot \exp(-\tau_0 \cdot \sec\theta) \tag{4}$$

and

$$T_{B,\mathrm{atm}}(\theta) = \sec\theta \int_0^\infty \kappa_a(z') \cdot T(z') \exp\left(-\tau(0,z') \cdot \sec\theta\right) dz' \tag{5}$$

where $T_{\mathrm{extra}}$ is the extraterrestrial brightness temperature (Kelvin), which is ∼2.7 K, $\tau_0$ is the total zenith opacity (Np), $\theta$ is the zenith angle, $\kappa_a$ is the atmospheric absorption coefficient $(\mathrm{Np} \cdot \mathrm{m}^{-1})$, $T$ is the temperature profile (Kelvin), and $\tau(0, z')$ is the optical thickness of the atmosphere between the surface and height $z'(\mathrm{Np})$. Given the atmospheric temperature, pressure, and water vapor density, the sky brightness temperatures can be calculated based on the 1962 U.S. Standard Atmosphere [8]. At C-band, the sensitivity of sky brightness to changes in atmospheric conditions can be ignored due to the high atmospheric transparency [8].

The sources of error using EC include the measurement errors due to the antenna sidelobes, $\varepsilon_{\mathrm{sl}}$, the insertion loss variability of the radiometer switches, $\varepsilon_{\mathrm{sw}}$, and the uncertainty in the physical temperature measurements of the absorber $\varepsilon_{\mathrm{at}}$. While errors due to measurement of antenna efficiency contribute to errors in antenna noise temperatures, these errors are removed in the correction to scene brightness temperatures because the calibration targets are all external to the antenna. The effect of these errors using UFCMR and TMRS-3C will be discussed in Section V.

### B. TC Calibration

$T_{B,\mathrm{sky}}$ can be obtained by TC assuming a horizontally stratified atmosphere [19] and [25] as

$$T_{B,\mathrm{sky}} = T_{\mathrm{extra}} \cdot \exp\left[-A(\theta) \cdot \tau\right] + T_{\mathrm{atm}} \cdot \left(1 - \exp\left[-A(\theta) \cdot \tau\right]\right) \tag{6}$$

where $A$ is the airmass at zenith angle $\theta$, $\tau$ is the atmospheric opacity (Np), and $T_{\mathrm{atm}}$ is the mean atmospheric temperature (Kelvin). For UFCMR and TMRS-3C, the antenna temperature is linearly related to the output voltage such that

$$\frac{V_{\mathrm{out,sky}} - V_{\mathrm{out,abs}}}{V_{\mathrm{out,abs}} - V_{\mathrm{ofst}}} = \frac{T'_{A,\mathrm{sky}} - T'_{A,\mathrm{abs}}}{T'_{A,\mathrm{abs}} - T_{\mathrm{rec}}} \tag{7}$$

where $V_{\mathrm{ofst}}$ is the system offset voltage when the system input noise temperature is 0 K $(T_{\mathrm{sys}} = T'_A + T_{\mathrm{rec}})$, $T'_{A,\mathrm{sky}}$ and $T'_{A,\mathrm{abs}}$ are the apparent antenna temperatures for the sky and absorber measurements, respectively (Kelvin), and $T_{\mathrm{rec}}$ is the receiver noise temperature (Kelvin). The equations for $S$ and $I$ are the same as (2) and (3), with $T_{B,\mathrm{sky}}$ estimated by the radiative transfer equation using the least-squares technique from 0° to 45°. The atmospheric temperature was approximated by the air temperature at the Earth's surface [19].

The sources of error using TC include $\varepsilon_{\mathrm{sl}}$, $\varepsilon_{\mathrm{sw}}$, and $\varepsilon_{\mathrm{at}}$, similar to those in EC. Errors in antenna noise temperatures due to uncertainty in the antenna efficiency are removed in the correction to scene brightness temperatures.

### C. Internal Calibration

IC uses an internal matched load or a fixed-temperature source, such as a noise diode, inside the radiometer as the hot target. The cold target is the sky measurement at 15° for UFCMR and at 0° for TMRS-3C. The $S$ and $I$ using IC are

$$S = \frac{T_{B,\mathrm{sky}} \cdot \eta + T_{\mathrm{ant,sky}} \cdot (1-\eta) - T_{\mathrm{cal}}}{V_{\mathrm{out,sky}} - V_{\mathrm{out,cal}}} \tag{8}$$

$$I = T_{\mathrm{cal}} - S \cdot V_{\mathrm{out,cal}} \tag{9}$$

where $T_{\mathrm{cal}}$ is the physical temperature of the matched load (Kelvin), $\eta$ is the antenna efficiency, $V_{\mathrm{out,cal}}$ is the output voltage when switched to the matched load at $T_{\mathrm{cal}}$ (volts), and $T_{B,\mathrm{sky}}$ is estimated, similar to EC [8].

The sources of error using IC include the $\varepsilon_{\mathrm{sl}}$ and $\varepsilon_{\mathrm{sw}}$, similar to those in EC, the error due to the uncertainty in the antenna efficiency estimation $\varepsilon_{\mathrm{ae}}$ and the uncertainty in the physical temperature measurements of the internal load $\varepsilon_{\mathrm{lt}}$.

### D. LEM

For an open calm water surface, the brightness temperatures observed by a microwave radiometer can be modeled as

$$T_{B,p} = \Gamma_p \cdot T_{B,\mathrm{sky}} + (1 - \Gamma_p) \cdot T_{\mathrm{water}} \tag{10}$$

where $\Gamma_p$ is the reflectivity at polarization $p$, and $T_{\mathrm{water}}$ is the physical temperature of water (Kelvin). $T_{B,\mathrm{sky}}$ is ∼5 K for C-band. The reflectivity of the specular water surface is determined by the incidence angle [26] and the dielectric constant of the water. The empirical models used for the dielectric constant of pure water can be found in [27] and [28].

## V. Results and Discussion

The calibration data from MicroWEXs and REBEX-10 provided a unique opportunity to compare the performance of two C-band radiometers with similar design in different environmental conditions. During each experiment, the radiometers were maintained at constant temperatures with 0.1 K standard deviation at the RF circuitry. Table II shows the means and the standard deviations of the calibration curves at H-pol during MicroWEXs and REBEX-10. These included 25 data points during MicroWEXs, as well as 80 points for EC and IC, and two points for TC during REBEX-10. IC produced the most consistent calibration curves in terms of the lowest standard deviations of the slopes, although the differences among the calibration techniques were not significant.

Fig. 1(a)–(d) shows the gain fluctuations of the calibration curves for MicroWEXs and REBEX-10. The mean absolute difference (MAD) between the slopes of EC and IC was 2.8 K/V during MicroWEXs. The difference between the slopes of TC and EC was 4.4 K/V, and the difference between the slopes of TC and IC was 3.6 K/V during MicroWEXs. The MADs for REBEX-10 were not calculated because there were only two TC measurements. During MicroWEXs, the EC and IC calibration curves were closer to each other, while TC produced slightly dissimilar results from EC and IC. This was primarily

TABLE II
MEAN AND STANDARD DEVIATION OF THE SLOPES ($S$) AND INTERCEPTS ($I$) FOR THE H-POL CALIBRATION CURVE DURING MICROWEXs (MWS) AND REBEX-10 (RB)

| Unit: S [K/v] and I [K] | EC | | IC | | TC | |
|---|---|---|---|---|---|---|
| | Mean | Std. | Mean | Std. | Mean | Std. |
| S MW1 | 189.37 | 3.81 | 188.62 | 2.00 | 182.48 | 3.12 |
| S MW2 | 172.91 | 7.18 | 173.94 | 2.88 | 173.29 | 3.74 |
| S MW3 | 163.84 | 5.64 | 165.66 | 3.09 | 164.19 | 4.48 |
| S RB | 152.35 | 3.68 | 152.62 | 0.84 | 150.34 | 3.40 |
| I MW1 | -131.10 | 5.37 | -130.37 | 3.66 | -116.24 | 6.58 |
| I MW2 | -98.41 | 3.41 | -99.44 | 7.14 | -98.01 | 4.88 |
| I MW3 | -86.02 | 18.19 | -87.34 | 16.60 | -83.66 | 19.20 |
| I RB | -69.18 | 5.38 | -69.47 | 4.23 | -65.70 | 6.68 |

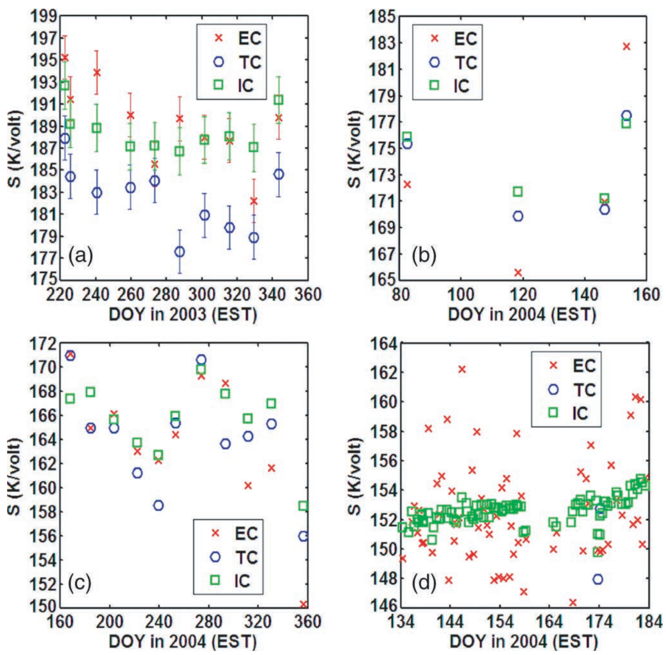


Fig. 1. Slopes for the calibration curve at H-pol during (a) MicroWEX-1, (b) 2, (c) 3, and (d) REBEX-10. RMSE of EC = 1.20, TC = 1.84, and IC = 1.10 K/V. For clarity of the figures, only Fig. 1(a) shows the error bars.

because at C-band, TC is based on multiple measurements with small differences in brightness temperatures ($T_B$'s) of the sky, compared to measurements at higher frequencies at which the differences are larger. Due to the high atmospheric transparency, the utility of TC at C-band was reduced. Applying the calibration curves over the output voltages for the terrains observed during MicroWEXs and REBEX-10, the MAD of the calibrated $T_B$'s using the three calibration techniques was 1.14 K. Table III gives the root-mean-square errors (RMSEs) estimates in the accuracy of observed $T_B$'s using UFCMR and TMRS-3C due to $\varepsilon_{\rm ae}$, $\varepsilon_{\rm sl}$, $\varepsilon_{\rm sw}$, $\varepsilon_{\rm at}$, and $\varepsilon_{\rm lt}$, as mentioned in Section IV. The RMSE of EC, TC, and IC are 1.20, 1.84, and 1.10 K/V, respectively.

To assess the accuracy of the calibration, we observed $T_B$'s of a calm lake at different incidence angles between 20° and 55° during REBEX-10. The RMSEs due to antenna sidelobes during the lake observations were 0.28, 0.26, 0.25, 0.25, and 0.24 K at incidence angles of 23°, 30°, 32°, 40°, and 55°, respectively. These RMSEs are included in the error bars shown in Fig. 2(a) and (b). Observed $T_B$'s were compared with those of a smooth water surface simulated by LEM (Fig. 2). We used

TABLE III
RMSE ESTIMATION FOR THE OPERATION AND CALIBRATION OF UFCMR AND TMRS-3C

| Symbol | Source | Value (K) |
|---|---|---|
| $\varepsilon_{ae}$ | Antenna Efficiency | < 0.14 |
| $\varepsilon_{sl}$ | Antenna Sidelobes (Incidence angle 0° to 45°) | 1.06 to 1.75 |
| $\varepsilon_{sw}$ | Radiometer Switch | < 0.25 |
| $\varepsilon_{at}$ | Absorber Temperature Measurements | < 0.50 |
| $\varepsilon_{lt}$ | Load Temperature Measurements | < 0.10 |

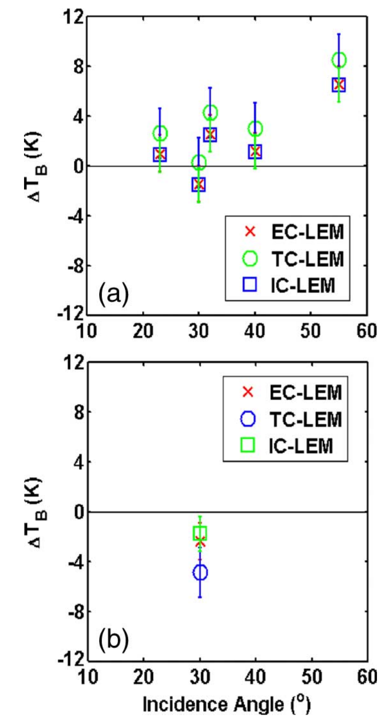


Fig. 2. Comparison of differences between the REBEX-10 observed and LEM simulated brightness temperatures ($\Delta T_B$) (a) at H-pol on DOY 173 and (b) at H-pol on DOY 174. The total RMSE between observed and simulated values are 1.46, 2.20, and 1.39 for EC, TC, and IC, respectively.

two dielectric models for pure water, [27], [28] and found that the MADs between the simulated LEM $T_B$'s were insignificant at ~0.0095 K. The uncertainty in the measurements of physical temperature of water was ±3.0 K resulting in an RMSE of 0.8 K at H-pol in the simulated $T_B$'s. The mean absolute errors (MAE) between the observed and modeled $T_B$'s at H-pol were 2.50 ±1.46, 3.90 ±2.02, and 2.40 ±1.39 K for EC, TC, and IC, respectively. For soil moisture applications, an accuracy of about 2 K at C-band is adequate [29].

## VI. CONCLUSION

The calibration experiments during the MicroWEXs and REBEX-10 were designed to assess the calibration consistency of two C-band radiometers with similar design. We compare the three most widely used techniques EC, TC, and IC to understand their performance for long-term soil moisture studies using ground-based C-band radiometers. Even though IC produced the most consistent calibration curves, the differences among the three calibration techniques were not significant. Applying the calibration curves over the range of output voltages observed during the MicroWEXs and REBEX-10, the MAD of the $T_B$'s calibrated among the three calibration techniques was 1.14 K. The absolute accuracy of calibration techniques was investigated by comparing the observed and modeled $T_B$'s of a calm lake. The MAE between the observed and modeled $T_B$'s were 2.50 $\pm$1.46, 3.90 $\pm$2.02, and 2.40 $\pm$1.39 K at H-pol for EC, TC, and IC, respectively. Due to the high atmospheric transparency, the utility of TC at C-band is greatly reduced. Because IC was found to have a MAE of $\sim$2 K, suitable for soil moisture applications, and was consistent during our experiments under significantly different environmental conditions, it can be used to augment less frequent calibrations obtained by the EC or TC techniques.

## ACKNOWLEDGMENT

The authors would like to thank the anonymous reviewers for their constructive comments and suggestions that improved this paper. The authors would also like to thank T. Lin, J. Casanova, M.-Y. Jang, L. Miller, and O. Lanni for their support during the MicroWEXs, the PSREU Research Coordinator J. Boyer and his team for providing excellent management of the study fields, and M. Dukes (University of Florida) for providing the measurements of air pressure and temperature used for calibrating the UFCMR.

## REFERENCES

[1] T. J. Jackson and P. E. O'Neill, "Attenuation of soil microwave emission by corn and soybean at 1.4 and 5 GHz," *IEEE Trans. Geosci. Remote Sens.*, vol. 28, no. 5, pp. 978–980, Sep. 1990.

[2] T. J. Jackson, P. E. O'Neill, and C. T. Swift, "Passive microwave observation of diurnal surface soil moisture," *IEEE Trans. Geosci. Remote Sens.*, vol. 35, no. 5, pp. 1210–1222, Sep. 1997.

[3] J. Judge, J. F. Galantowicz, and A. W. England, "A comparison of ground-based and satellite-borne microwave radiometric observations in the Great Plains," *IEEE Trans. Geosci. Remote Sens.*, vol. 39, no. 8, pp. 1686–1696, Aug. 2001.

[4] J. Shi, K. S. Chen, Q. Li, T. J. Jackson, P. E. O'Neill, and L. Tsang, "A parameterized surface reflectivity model and estimation of bare-surface soil moisture with L-band radiometer," *IEEE Trans. Geosci. Remote Sens.*, vol. 40, no. 12, pp. 2674–2686, Dec. 2002.

[5] F. Lemaitre, J. C. Poussiere, Y. H. Kerr, M. Dejus, R. Durbe, P. Rosnay, and J. C. Calvet, "Design and test of the ground-based L-band radiometer for estimating water in soil (LEWIS)," *IEEE Trans. Geosci. Remote Sens.*, vol. 42, no. 8, pp. 1666–1676, Aug. 2004.

[6] K. Schneeberger, C. Stamm, C. Matzler, and H. Fluhler, "Ground-based dual-frequency radiometry of bare soil at high temporal resolution," *IEEE Trans. Geosci. Remote Sens.*, vol. 42, no. 3, pp. 588–595, Mar. 2004.

[7] A. Memmo, E. Fionda, T. Paolucci, D. Cimini, R. Ferretti, S. Bonafoni, and P. Ciotti, "Comparison of MM5 integrated water vapor with microwave radiometer, GPS, and radiosonde measurements," *IEEE Trans. Geosci. Remote Sens.*, vol. 43, no. 5, pp. 1050–1058, May 2005.

[8] F. T. Ulaby, R. K. Moore, and A. K. Fung, *Microwave Remote Sensing—Active and Passive*, vol. I. Norwood, MA: Artech House, 1981, pp. 369–396.

[9] N. Skou, *Microwave Radiometer Systems: Design and Analysis*. Norwood, MA: Artech House, 1989, pp. 13–19.

[10] E. Njoku, J. M. Stacey, and F. T. Barath, "The Seasat Scanning Microwave Radiometer (SMMR): Instrument description and performance," *IEEE J. Ocean. Eng.*, vol. OE-5, no. 2, pp. 100–115, Apr. 1980.

[11] C. S. Ruf, "Detection of calibration drifts in spaceborne microwave radiometers using a vicarious cold reference," *IEEE Trans. Geosci. Remote Sens.*, vol. 38, no. 1, pp. 44–52, Jan. 2000.

[12] C. S. Ruf and J. Li, "A correlated noise calibration standard for interferometric, polarimetric, and autocorrelation microwave radiometers," *IEEE Trans. Geosci. Remote Sens.*, vol. 41, no. 10, pp. 2187–2196, Oct. 2003.

[13] C. S. Ruf, S. J. Keihm, and M. A. Janssen, "TOPEX/Poseidon Microwave Radiometer (TMR). I. Instrument description and antenna temperature calibration," *IEEE Trans. Geosci. Remote Sens.*, vol. 33, no. 1, pp. 125–137, Jan. 1995.

[14] C. S. Ruf, S. J. Keihm, B. Subramanya, and M. A. Janssen, "TOPEX/POSEIDON Microwave Radiometer performance and in-flight calibration," *J. Geophys. Res.*, vol. 99, no. C12, pp. 24 915–24 926, 1994.

[15] P. Bonnefond, B. Haines, G. Born, P. Exertier, S. Gill, G. Jan, E. Jeansou, D. Kubitscheck, O. Laurain, Y. Menard, and A. Orsoni, "Calibrating the Jason-1 measurement system: Initial results from the Corsica and Harvest verification experiments," *Adv. Space Res.*, vol. 32, no. 11, pp. 2135–2140, 2003.

[16] I. Corbella, A. J. Gasiewski, M. Klein, V. Leuski, A. J. Francavilla, and J. R. Piepmeier, "On-board calibration of dual-channel radiometers using internal and external references," *IEEE Trans. Microw. Theory Tech.*, vol. 50, no. 7, pp. 1816–1820, Jul. 2002.

[17] H. Pham, E. J. Kim, and A. W. England, "An analytical calibration approach for microwave polarimetric radiometers," *IEEE Trans. Geosci. Remote Sens.*, vol. 43, no. 11, pp. 2443–2451, Nov. 2005.

[18] B. Deuber, N. Kampfer, and D. G. Feist, "A new 22-GHz radiometer for middle atmospheric water vapor profile measurements," *IEEE Trans. Geosci. Remote Sens.*, vol. 42, no. 5, pp. 974–984, May 2004.

[19] Y. Han and E. R. Westwater, "Analysis and improvement of tipping calibration for ground-based microwave radiometer," *IEEE Trans. Geosci. Remote Sens.*, vol. 38, no. 3, pp. 1260–1276, May 2000.

[20] K. Al-Ansari, P. Garcia, J. M. Riera, A. Benarroch, D. Fernandez, and L. Fernandez, "Calibration procedure of a microwave total-power radiometer," *IEEE Microw. Wireless Compon. Lett.*, vol. 12, no. 3, pp. 93–95, Mar. 2002.

[21] D. Cimini, E. R. Westwater, Y. Han, and S. J. Keihm, "Accuracy of ground-based microwave radiometer and balloon-borne measurements during the WVIOP2000 field experiment," *IEEE Trans. Geosci. Remote Sens.*, vol. 41, no. 11, pp. 2605–2615, Nov. 2003.

[22] K. C. Tien, J. Judge, L. W. Miller, and O. Lanni, *Field Data Report for the First Microwave Water and Energy Balance Experiment (MicroWEX-1) July 17–December 16, 2003*, Gainesville, FL: Center for Remote Sensing, Univ. Florida, 2005. [Online]. Available: http://edis.ifas.ufl.edu/AE288

[23] T. Lin, J. Judge, K. C. Tien, J. J. Casanova, M. Jang, O. Lanni, L. W. Miller, and F. Yan, *Field Observations During the Third Microwave Water and Energy Balance Experiment (MicroWEX-3) June 16–December 21, 2004*, Gainesvile, FL: Center for Remote Sensing, Univ. Florida, 2005. [Online]. Available: http://edis.ifas.ufl.edu/AE361

[24] J. Judge, J. J. Casanova, T. Lin, K. C. Tien, M. Jang, O. Lanni, and L. W. Miller, *Field Observations During the Second Microwave Water and Energy Balance Experiment (MicroWEX-2) March 17–June 3, 2004*, Gainesville, FL: Center for Remote Sensing, Univ. Florida, 2005. [Online]. Available: http://edis.ifas.ufl.edu/AE360

[25] M. A. Janssen, *Atmospheric Remote Sensing by Microwave Radiometry*. New York: Wiley, 1993, pp. 259–334.

[26] L. A. Rose, W. E. Asher, S. C. Reising, P. W. Gasier, K. M. St. Germain, D. J. Dowgiallo, K. Horgan, G. Farquharson, and E. J. Knapp, "Radiometric measurements of the microwave emissivity of foam," *IEEE Trans. Geosci. Remote Sens.*, vol. 40, no. 12, pp. 2619–2625, Dec. 2002.

[27] L. A. Klein and C. T. Swift, "An improved model for the dielectric constant of sea water at microwave frequencies," *IEEE Trans. Antennas Propag.*, vol. AP-25, no. 1, pp. 104–111, Jan. 1977.

[28] T. Meissner and F. J. Wentz, "The complex dielectric constant of pure and sea water from microwave satellite observations," *IEEE Trans. Geosci. Remote Sens.*, vol. 42, no. 9, pp. 1836–1849, Sep. 2004.

[29] J. C. Calvet, A. Chanzy, and J. P. Wigneron, "Surface temperature and soil moisture retrieval in the Sahel from airborne multifrequency microwave radiometry," *IEEE Trans. Geosci. Remote Sens.*, vol. 34, no. 2, pp. 588–600, Mar. 1996.